

# CRASHWORTHINESS OF ISOFIX AND LATCH CHILD RESTRAINT SYSTEMS IN TRANSPORT CATEGORY AIRCRAFT

**Adam Shrimpton, Cees Bil, Graham Clark**  
**School of Aerospace, Mechanical and Manufacturing Engineering,**  
**RMIT University, Melbourne, AUSTRALIA**

## Abstract

This paper describes progress in a research project which aims to analyse the crashworthiness of automotive child restraints in a typical transport category aircraft seating configuration using a numerical dynamic analysis. The dynamic behaviour of child restraints and especially their effect on the safety of other passengers is not well known. The advent of new child restraint installation methods has elevated the need for a fast and reliable tool to enable the assessment of the crashworthiness of seating configurations involving child restraints. The numerical model is based on the configurations used in physical dynamic tests conducted by the Civil Aviation Safety Authority (CASA) in Australia. The overall objectives are to:

1. Develop validated numerical models of the aircraft seat and relevant child restraints.
2. Use the models to conduct a parametric crashworthiness analysis of various seating configurations.
3. Report on the findings of this research in a form suitable for supporting development of new regulator and advisory material as well as input to Standards Australia.

Efforts in the first phase of the project have focused on the creation of a validated model of the same aircraft seating arrangement used by CASA in physical tests. This involved the assessment of each component of the seat structure in terms of both its influence on the dynamic performance of the structure as whole and also its effect on the dynamic behaviour of the seat occupant. Relevant seat components were then digitised and incorporated into a

simplified seat assembly model. Relevant material properties were found by means of laboratory testing.

## 1 Introduction

The use of automotive child restraints in aircraft has been found to significantly increase the safety of an infant passenger during a crash[1]. However, for several reasons - most of them relating to operational difficulties - their use in the air transport environment is not common. Instead, infants may be lap-held with a supplementary loop belt which however is not optimal from a crash safety point of view[6]. If



Figure 1 Rear passenger impact with child restraint system installed [2].

the use of new child restraints in aircraft is to become more common, their impact on safety for the child and other passengers must be investigated. The ISOFIX and LATCH type child restraints have been shown to overcome many of the difficulties typically associated with child restraint use in aircraft[2]. However, sled tests established that their implementation may have negative consequences for the safety of an adult passenger seated behind the child restraint[3], as shown in Fig. 1. The presence of

a rigid infant restraint system prevents the seatback from breaking forward in the event of a crash causing severe injuries to the passenger seated behind it. This requires solutions in design and operational use of child restraint systems in aircraft.

Experimental research has been carried out using a typical economy class airline seating configuration involving various child restraints[3]. This research identified the need for an additional analytical approach. One solution is the creation of a customisable numerical model into which different child restraints and occupants, both child and adult, may be placed and subjected to various loading conditions. This would allow different seating configurations and loading scenarios to be analysed in less time and with less cost.

## 2 Scope and Objectives

The objective of this research is the development of a numerical crashworthiness model of an airline seating configuration involving child restraints. Where possible, the model is being designed in such a way as to be customisable and adaptable to future research applications. The model will be validated to CASA's specification against experimental data provided by CASA. The model will then be used to conduct a parametric analysis of the seating configuration in an effort to identify those combinations which are most hazardous to occupant safety and those which are most beneficial. Parameters include seat pitch, occupant size, child restraint anchorage stiffness, material properties and joint behaviour. This research will be used by CASA in creating advisory material.

The scope of this research includes only the aircraft seat type and basic configuration used to date in experimental research[3]. Injury levels to both adult and child occupants are considered, as well as child restraint anchor loads and aircraft seat attachment loads.

## 3 Analysis Methods

### 3.1 Introduction

The model developed as part of this research project is based on the configurations used in physical dynamic tests. In these tests, two rows of two typical economy class airline seats were fixed to a horizontal crash simulator and subjected to an acceleration pulse. During the tests, numbering sixteen in total, each of the four seats was occupied by an anthropomorphic test device (ATD). Both adult and child ATDs were used, with the child ATDs being restrained by an automotive child restraint, the aircraft lap belt, or a supplemental belt on the lap of a 'parent' ATD. Data from these tests is in the form of high-speed video footage and the output of various sensors integral to the ATDs or attached to the seat structure. Figure 1 shows a still image from the high speed video footage.

The aircraft seats used in physical testing by CASA are B/E Aerospace model BA3.4-2-41. They are labelled as being rated to 9.0 G forward load.

### 3.2 Software selection

There are several commercially available software options in the field of crashworthiness. The two main codes considered were LS-Dyna and MADYMO. Both are widely used in research of this kind, though MADYMO was ultimately selected for its emphasis on occupant safety and its library of included ATD models. MADYMO is produced by TNO Automotive Safety Solutions of the Netherlands.

MADYMO is a combined dynamic finite element (FE) and multibody (MB) dynamics code. Models may consist purely of FE, multibody objects or a combination of the two. FE and multibody objects may be made to interact through joints or contact definitions.

### 3.3 Testing, verification and validation

Where practicable, each material and component model is tested, verified and validated against physical test data. This involves conducting a controlled laboratory test

of a given material or component followed by a numerical simulation of the laboratory test.

The completed model will be validated numerically against the experimental data from sled tests. Validation parameters include all ATD sensor output, and, where available, lap belt tension and restraint anchor loads. At that stage the Sprague and Geers error metric [4] will be used to validate sensor output signals in terms of phase and magnitude, and this will be supported by visual validation against high-speed video footage.

### **3.4 Model creation**

#### *3.4.1 System simplification*

One of the requirements of the model is that the end product will be useful in conducting a parametric analysis of various seating configurations. This means that parameters such as seat pitch, material properties and joint behaviour must be able to be altered without significant effort. Another effect of this requirement is that the computational time required by the model should not be so great as to be prohibitive in conducting a parametric analysis. For these reasons a high-fidelity finite element model of the aircraft seat structure would not be appropriate for this application. Therefore some simplification of the seat structure has been required.

High-speed video footage and visual inspection of the post-crash seat structure were used to identify those components that are critical to the dynamic behaviour of the seat and its occupants. These are generally components which undergo a high degree of deformation under crash loading. Examples include the tray table, the seat back frame and associated break-over limiting device, the seat base cushion, the lap belt and the two lateral tubes form part of the seat substructure. For the model to be useful, these components must be modelled in a way such that their behaviour in the numerical model matches reality as closely as possible. Components such as the legs may be modelled as rigid or semi-rigid components with simplified geometry while others such as the components comprising the seat back break-over limiting mechanism may be replaced by a

numerical joint having the same rotational stiffness as the mechanism itself. These measures reduce model complexity, making the task of modifying the model simpler and significantly reducing computational requirements.

#### *3.4.2 Geometry input, simplification and meshing*

Aircraft seat geometry data was obtained from post-test seats and also from undamaged seats supplied by Qantas. The child restraint geometry obtained thus far is from the Britax *DuoPlus* and *Cosy-Tot* restraints. Geometry data was acquired by means of a 3D optical scanner, an articulated-arm type coordinate measurement machine, Vernier calipers and tape measure.

Geometry was imported into the Altair Hypermesh application for surface creation, finite element meshing and some pre-processing. Where appropriate, parts such as the seatback frame pictured above were simplified by making the geometry more uniform and, in this case, symmetrical. This was done in order to reduce mesh complexity and facilitate joint creation and modification.

#### *3.4.3 Model pre-processing*

The MADYMO software package includes an XML-based pre-processor called XMADGic. The input deck generated by Hypermesh is imported into XMADgic for the addition of joints, constraints and contact definitions and the assignment of section and material properties. ATD models are inserted, positioned and secured.

##### *3.4.3.1 Material models*

The MADYMO solver uses a library of approximately 30 different material models, ranging from linear elastic isotropic materials to composites, fabric and foam. Different material types require their properties to be specified in different ways and also may be limited to certain element types. For example, a linear elastic isotropic material may be defined by only its Young's modulus, density and Poisson ratio. It is applicable to most element types.

Meanwhile, the foam material model must be defined using a loading curve and is only applicable to solid elements.

#### *3.4.3.2 Joint models*

There are two different methods of creating joints between entities in MADYMO; finite element constraints and kinematic joints. Which method is appropriate depends on the nature of the joint and the entity type (MB or FE). Finite element entities may be constrained to one another using a finite element constraint. This constraint may be fully rigid or alternatively may connect only specific degrees of freedom. Constraints of this type cannot have any joint properties such as friction applied. Where the constraint is rigid, a spot-weld element may also be used.

Kinematic joints may be created between any combination of entity types. The attachment point of a joint to a finite element entity must be comprised of rigid elements. There are several different types of kinematic joints; fixed brackets, rotational, translational and combinations thereof. Kinematic joints may have characteristics such as friction, load-displacement curves and hysteresis.

#### *3.4.3.3 Contact definitions*

MADYMO, like most solvers of its type, does not automatically calculate and apply forces generated by contact between two entities. Instead, the user must define the contact; both in terms of what pairs of entities to check for contact and also how to calculate and apply the resulting contact force. Careful selection of entities to include in contact definitions will result in a shorter solver run time than if unnecessary or insignificant contacts are defined.

The method by which contact forces are calculated must be specified by the user. Each contact definition must have at least one entity set designated the 'master' and may optionally have a second set designated the 'slave' for the purposes of contact force calculation. Multibody surfaces may have a force-displacement or stress-strain curve associated with them to enable the calculation of contact forces. Where

one of the entities is a set of finite elements, contact forces may be calculated based on the kinematic response of those elements.

#### *3.4.3.4 ATD models*

The MADYMO package includes a comprehensive library of validated human and ATD models[5]. Human models are generally available as facet models and finite element models, while ATD models are generally available as ellipsoid models and facet models. This research is primarily concerned with ATD models and will implement the ellipsoid model versions of the Hybrid III and TNO P series ATDs used by CASA. The ellipsoid models are chosen here for their ease of implementation and modest computational requirements.

#### *3.4.4 Solver*

The MADYMO solver supports Windows, Linux and UNIX platforms. Input decks are validated on a Windows desktop PC before being transferred to the RMIT High Performance Computing (HPC) system for processing. The HPC resource used is a single Sun X2200 M2 node comprising 2 quad-core AMD Opteron 2356 2.3 GHz CPUs and 32 GB RAM.

The validation build of the aircraft seat model discussed later in this report requires approximately 1.25 hours of real time, or approximately 11 hours of CPU time, to solve for a 200 ms period. It is estimated that the completed model with four ellipsoid ATD models will require approximately six hours to solve for the same time period.

#### *3.4.5 Model output*

If requested by the user, MADYMO generates visual as well as numerical output at customisable time intervals. Examples of numerical output include signal data from user-specified accelerometers or time-histories of restraint forces, body positions, contact forces and element data. Signal data may have one of a variety of filters applied. MADYMO also calculates the values of various injury values such as head and neck injury criteria.

## 4 Initial Results

### 4.1 Material and component testing and validation

#### 4.1.1 Introduction

The development of a high fidelity model requires detailed modeling of the seat frame, foam material, break-over device, lap belt material and lateral seat structure. Currently, the modeling of the Foam (LRGR45, LD24FR, AF60, cushion) is complete, and a quasi-static test of the tray table is complete, with a dynamic test scheduled.

#### 4.1.2 Foam material

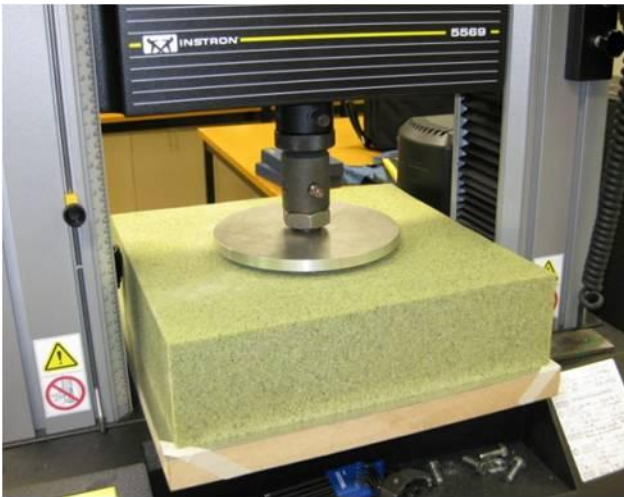


**Figure 2** LRGR45 foam sample installed in test machine

The high-speed footage from the CASA tests indicates that the seat base cushion has a significant effect on the dynamic behaviour of both child restraints and ATDs. One sample of each of the three types of foam which constitute the seat base cushion was obtained from the manufacturer for testing. A quasi-static test was developed based on ASTM D3574-05 *Standard Test Methods for Flexible Cellular Materials – Slab, Bonded and Molded Urethane Foams*. A flat circular indenter of 200 mm diameter was installed in an Instron 5569 mechanical testing machine with a 25 kN load cell installed. Each of the three 380 mm x 380 mm x 100 mm foam samples and also a complete seat cushion were compressed to 10% of their original thickness at rates of 125, 250 and 500 mm per minute. The test setup is shown in Fig. 2. This test regime

arrived at a set of data that displays the different strain-rate dependencies of the three types of foam used, an important material property in the context of dynamic modelling.

The three foams tested were LRGR45, AF60 and LD24FR produced by Dunlop Foams. LRGR45 and AF60 are open-cell polyurethane foams, while LD24FR is a closed-cell low density polyethylene foam. Of *the* three foams tested, LRGR45 exhibits the greatest strain-rate dependency and is colloquially termed ‘memory foam’. It is used in the upper layer of the seat base cushion. Fig. 3 shows the force during the loading portion of the test cycle at 80% strain for both LRGR45 and AF60 each at three different strain rates. The effects of strain rate dependency are apparent even at these quasi-static loading rates.

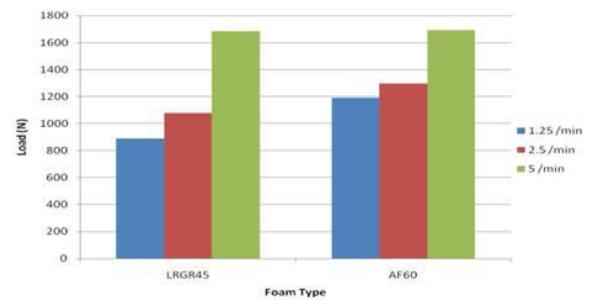


**Figure 3** Load at 80% strain for LRGR45 and AF60 at strain rates of 1.25, 2.5 and 5 per minute

The force during the unloading portion of the test cycle was also measured in order to capture the effect of hysteresis. As expected, LRGR45 exhibited the greatest degree of hysteresis, with the indenter losing contact with the surface of the foam very early in the unloading portion of the cycle at all strain rates.

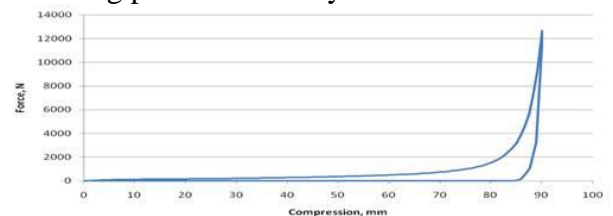


**Figure 4** Load curve for LRGR45 at 500 mm/min demonstrating hysteresis.

Fig. 4 shows the hysteresis exhibited by LRGR45 at a rate of 500 mm per minute. The

upper line is the force during loading, while the lower is the force during unloading.

The material models arrived at using these test results are to be validated in MADYMO using a simulation which exactly replicates the laboratory test conditions.

#### *4.1.3 Tray table*

The tray table is one of the primary points of impact for the ATD head. It undergoes highly dynamic loading and must be tested in a similar manner. To aid in the design of a dynamic test, a quasi-static three-point bending test was carried out using a hemispherical solid aluminium indenter of 150 mm diameter. It was found that the maximum bending moment able to be withstood by the tray table about the vertical axis as typically installed is approximately 88 Nm. This test was of the tray table only and did not include the supporting aluminium frame. A dynamic test making use of a drop-type impact rig is to be designed. A weighted indenter will be dropped onto the tray table which will be supported in three-point bending with an accelerometer affixed to the underside. The test will then be simulated in MADYMO in order to calibrate the impact response of tray table model.

#### *4.1.4 Break-over limiting device model*

The seatback break-over limiting device essentially consists of a pair of small thin steel plates attached to the hinge connecting the seat back to the seat frame. The plates are designed to buckle under the inertial load of the seatback under significant forward deceleration, controlling the forward rotation of the seat back. The motion of the seatback has a significant influence on the level of injury to a passenger seated in the seat to the rear; therefore it is critical that the effect of the break-over limiting device is modelled accurately.

A finite element model of the device itself, while possible, would unnecessarily add to the computational time required to run the model and also significantly increase the complexity involved if the device were to be incorporated into a future parametric study. Instead, the seatback is attached to the seat frame using

numerical revolute joints with a loading characteristic. This method requires a moment versus angular displacement curve, which will be measured using a mechanical testing machine in conjunction with a custom-fabricated fixture for fixing the break-over limiting device to the machine. The result will be a joint which behaves accurately, is computationally inexpensive and easily modifiable.

#### *4.1.5 Additional materials tests*

A sample of the lap belt material will be tested in order to find a load-extension curve for use in the MADYMO belt model, and a length of the material comprising the seatback frame will be placed in three-point bending to determine its Young's modulus.

Footage from the CASA tests and post-test inspection of the seat frames indicates that the lateral tubes undergo significant plastic deformation. In order to ascertain the properties of the specific aluminium alloy in question, a coupon tensile test will be carried out in the laboratory to determine the Young's modulus and yield stress of the material.

## **4.2 Initial build of aircraft seat model**

An initial build of the aircraft seat model has been completed for the purpose of verifying joint creation techniques and contact definitions. In an effort to minimise development time, the model comprises only the minimum number of components necessary for the task, i.e. one seatback assembly per row and only one ATD model. To date the model has undergone close to 100 revisions.

Until laboratory test data for critical parameters such as tray table impact response and seatback break-over limiting device behaviour are available, estimated values are being used in lieu and, as such, it would not be expected that the results generated by this model will correlate with experimental data. Developing this framework, however, will make it relatively simple to incorporate laboratory test data into the model and begin validation and calibration.

All seat structural components were

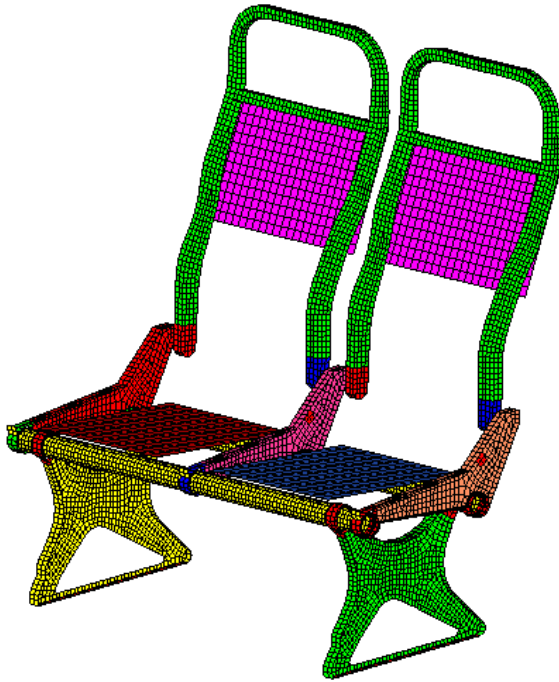


**Figure 5** Meshed seat model (cushions and fabric omitted for clarity)

meshed using three- or four-node shell elements as opposed to solid elements for reduced solver run-time. The average element size in the aircraft seat frame is approximately 10 mm, resulting in a total of approximately 24,000 shell elements in the two-by-two seat configuration (Fig. 5).

#### 4.2.1 Loading scenario

Unfortunately no physical test data exists for a baseline aircraft seat model where the occupant makes contact with the seat in front. Instead, CASA Phase II test 09/08 is being used as a substitute. In this test, two Hybrid III 50<sup>th</sup> percentile ATDs are seated behind two child restraints. One of these restraints, the *DuoPlus* is an aft-facing model which does not appear to greatly affect the forward rotation of the seatback. The acceleration field applied to the model is equivalent to that described by the sled accelerometer data from this test.

#### 4.2.2 Joints

The model makes use of two different joint methods. In the physical aircraft seat assembly,

there are ten clamp-type joints connecting the two lateral tubes to the two longitudinal legs and three longitudinal spreaders. In the numerical model, these joints are created by assigning the section of each part comprising a particular joint to a rigid material. These ten pairs of rigid parts are then constrained to one another using a rigid finite element constraint.

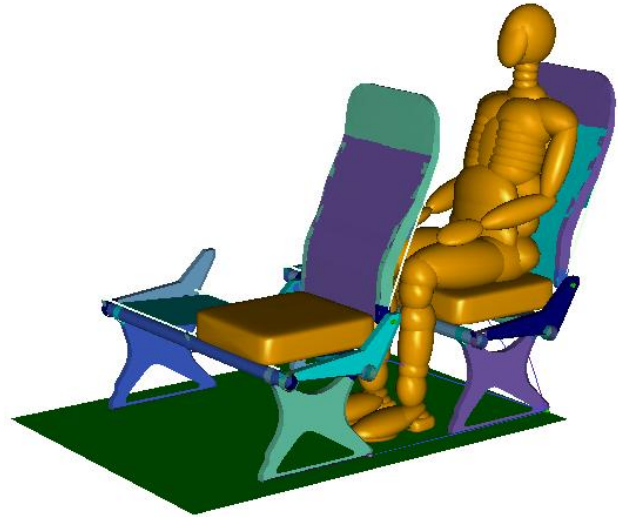


**Figure 6** Initial build of aircraft seat model with ATD occupant.

Using this method, all translations and rotations undergone by one half of a joint are directly transferred to the other half with minimal computational expenditure.

This method cannot be used for other joint types, however. In the case of the seatback hinges, a numerical revolute joint is used. This joint type allows the user to specify static and dynamic friction properties, as well as the option of joint loading and unloading curves. This latter option will be implemented once the seatback break-over limiting device load curve data are inserted. Until then, the joint is modelled with estimated static and dynamic friction values. Each side of the seatback is attached to the main seat frame using a separate hinge in order to model the twisting that the seatback frame undergoes during forward rotation.

#### 4.2.3 ATD model

A Hybrid III 50<sup>th</sup> percentile ellipsoid ATD model is installed in the aft seat and restrained by three belt elements (Fig. 6).

#### 4.2.4 Contacts

Table 1 lists the contacts defined in the initial build of the aircraft seat model.

**Table 1 - Contacts defined in initial aircraft seat model.**

Master Entity Set	Slave Entity Set	Contact Type	Characteristic
ATD pelvis, left & right femur	Seat base cushion	MB-MB	Slave
ATD left and right tibia	Aft lateral tube of forward seat	MB-FE	Kinematic
ATD head	Tray table of forward seat	MB-FE	Master
ATD shoes	Floor	MB-MB	Slave
Tray tables	Seat back frames	FE-FE	Kinematic
Seat base cushion	Seat pan fabric surface	FE-FE	Master

#### 4.2.5 Seat base cushion

Presently, the seat base cushion is approximated using an ellipsoid surface and the seat back cushion is omitted, since the inclusion of several thousand solid finite elements at this stage of the model development will slow progress significantly, and a validated foam material model has not yet been achieved. The seat base and back cushions will be meshed with eight-node solid elements approximately 20 mm in size.

#### 4.2.6 Results of initial build

As mentioned previously, the initial aircraft seat model requires approximately 1.25 hours of real time to solve using eight 2.3 GHz CPUs and 32

GB RAM. All contacts behave as expected and give sensible contact force results. The kinematic behaviour of all joints is as intended.

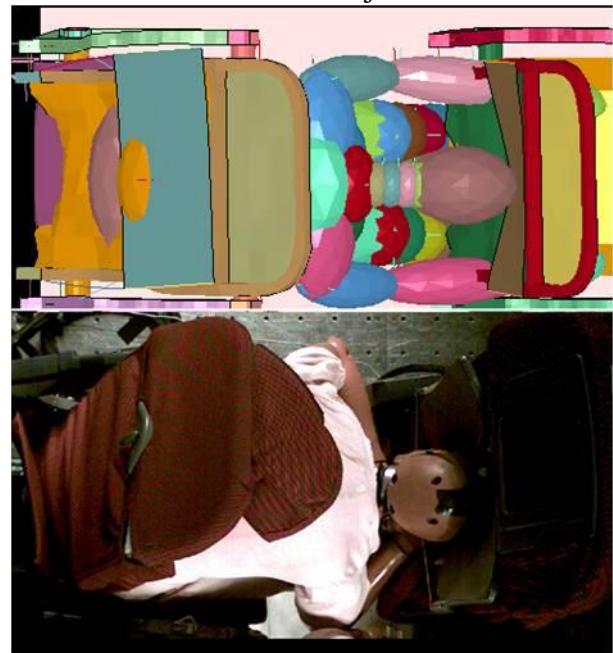


**Figure 7** Plan view of MADYMO model at 150 ms (top) and CASA test 09/08 at 135 ms (bottom).

The aft lateral tube of the aft seat assembly undergoes plastic deformation due to the ATD restraint load, while the aft lateral tube of the forward seat assembly undergoes plastic deformation at the point of impact of the ATD tibias. The kinematic response of the ATD, while slightly out of phase, correlates well with experimental results (Fig. 7).

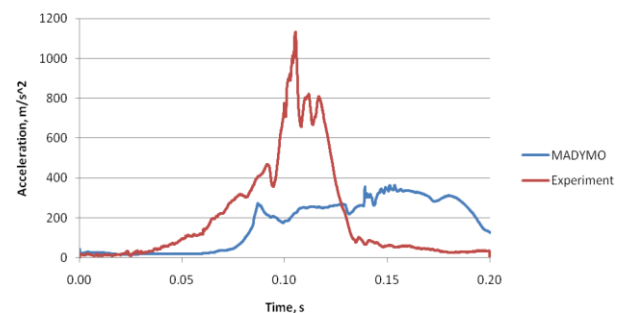


**Figure 8** Comparison of MADYMO and experimental head acceleration profiles.

Though not within the scope of this model build, some output data was compared with experimental results. As expected due the several approximations made in the initial



model build, sensor output data does not yet correlate with physical test results. Fig. 8 shows a comparison between the resultant head acceleration of the MADYMO ATD and the ATD seated behind the *DuoPlus* child restraint in CASA Phase II test 09/08. Both data sets have CFC1000 filters applied.

## **5 Conclusion**

Extensive dynamic sled tests conducted by CASA on child restraint systems in aircraft seats has demonstrated the need for more detailed analysis of seat and restraint system design combined with operational guidelines for child restraint system placement in the cabin. Tests have shown that the safety of surrounding passengers must be considered as well. This requires an analytical approach to the dynamic behaviour of passengers and seats in a crash environment. This tool will allow design modifications related to the seat design, material used and restraint system attachment. This paper has presented progress in a new research project sponsored by CASA to develop such a tool, with an initial selection of analysis tools, determination of material properties and seat/passenger modeling.

## **References**

- [1] Gowdy, V. and R. DeWeese, *The performance of child restraint devices in transport airplane passenger seats*. 1994, Civil Aeromedical Institute.
- [2] Olivares, G. and P. Amesar, *Implementation of ISOFIX and LATCH equipped automotive child restraint systems in an aircraft environment*. 2007, National Institute for Aviation Research.
- [3] Bathie, M., *An investigation of automotive child restraint installation methods in transport category aircraft*. 2007, Civil Aviation Safety Authority.
- [4] Sprague, M.A. and T.L. Geers, *Spectral elements and field separation for an acoustic fluid subject to cavitation*. *Journal of Computational Physics*, 2003. 184: p. 149-162.
- [5] TASS, *MADYMO Model Manual Release 7.1*. 2009, Delft, The Netherlands.
- [6] Civil Aviation Safety Authority, *Carriage and restraint of small children in aircraft*. 2002, CAAP 235-2(1)

## **Contact Author Email Address**

[a.shrimpton@student.rmit.edu.au](mailto:a.shrimpton@student.rmit.edu.au)

## **Copyright Statement**

The authors confirm that they, and/or their company or organization, hold copyright on all of the original material included in this paper. The authors also confirm that they have obtained permission, from the copyright holder of any third party material included in this paper, to publish it as part of their paper. The authors confirm that they give permission, or have obtained permission from the copyright holder of this paper, for the publication and distribution of this paper as part of the ICAS2010 proceedings or as individual off-prints from the proceedings.